J Mater Sci: Mater Med (2009) 20:229–234
DOI 10.1007/s10856-008-3573-4

3D polycaprolactone scaffolds with controlled pore structure using a rapid prototyping system

SuA Park · GeunHyung Kim · Yong Chul Jeon · YoungHo Koh · WanDoo Kim

Received: 25 May 2008 / Accepted: 18 August 2008 / Published online: 30 August 2008

Abstract Designing a three-dimensional (3-D) ideal scaffold has been one of the main goals in biomaterials and tissue engineering, and various mechanical techniques have been applied to fabricate biomedical scaffolds used for soft and hard tissue regeneration. Scaffolds should be biodegradable and biocompatible, provide temporary support for cell growth to allow cell adhesion, and consist of a defined structure that can be formed into customized shapes by a computer-aided design system. This versatility in preparing scaffolds gives us the opportunity to use rapid prototyping devices to fabricate polymeric scaffolds. In this study, we fabricated polycaprolactone scaffolds with interconnecting pores using a 3-D melt plotting system and compared the plotted scaffolds to those made by salt leaching. Scanning electron microscopy, a laser scanning microscope, micro-computed tomography, and dynamic mechanical analysis were used to characterize the geometry and mechanical properties of the resulting scaffolds and morphology of attached cells. The plotted scaffolds had the obvious advantage that their mechanical properties could be easily manipulated by adjusting the scaffold geometry. In addition, the plotted scaffolds provided more opportunity for cells to expand between the strands of the scaffold compared to the salt-leached scaffold.

S. Park · G. Kim · W. Kim
Bio-Mechatronics Team, Division of Nano-Mechanical System, Korea Institute of Machinery and Materials (KIMM), Daejeon, Korea

G. Kim (✉)
Department of Mechanical Engineering, Chosun University, GwangJu, Korea
e-mail: gkim@chosun.ac.kr

Y. C. Jeon · Y. Koh
ILSONG Institute of Life Science, Hallym Medical School, Hallym University, Anyang, Kyunggi-do, Korea

1 Introduction

Tissue engineered scaffolds are necessary to serve as bio-engineered constructs in guiding cell growth and tissue regeneration. The key requirements for an optimal three-dimensional (3-D) scaffold in tissue engineering consist of biocompatibility and biodegradability to enhance cell attachment, adequate mechanical properties to maintain the 3-D structure, appropriate surface chemistry and good hydrophilicity to promote cell adhesion, and high porosity with large interconnected pores to facilitate cell ingrowth and nutrient transportation [1, 2]. The scaffold porosity and pore size are especially important to the fabricating process. The formation of new tissue is greatly influenced by the porosity, pore size, and 3-D structure of the scaffold; a large pore structure is formed to deliver a sufficient number of cells, and the interconnected porosity allows for the easy diffusion of nutrients. Porous polymer scaffolds are promising materials because they offer valuable 3-D supports for cell growth and tissue formation.

The conventional techniques for 3-D scaffold fabrication, including salt leaching, gas foaming, fiber bonding, solvent casting, melt molding, and phase separation, have common limitations [3]. These technologies are unable to produce an interconnected structure for cell ingrowth or control the pore size for cell migration and diffusion. The scaffold architecture must be designed and fabricated to fit the needs of individual applications. Only the new rapid prototyping (RP) technology has the potential to solve these requirements. Various rapid prototyping techniques

use solid free-form fabrication (SFF) such as stereolithography (SLA), selective laser sintering (SLS), 3-D printing (3DP), and fused deposition modeling (FDM) [3–6]. Many different processing techniques have been developed to design and fabricate 3-D scaffolds for tissue engineered scaffolds [7–10]. Among the different RP technologies, stereolithography cannot be used for scaffold production due to the use of toxic resins. However, SFF can use a Bioplotter® derived from biodegradable polyesters such as polycaprolactone (PCL) without toxic solvents.

RP technology using computer-aided tissue engineering (CATE) can produce a well-defined internal and external shape with uniform porosity for cell ingrowth [11–16]. The Bioplotter® System can control the design factors including pore size and shape, porosity, strand orientation, nozzle size, strand distance, and interconnectivity. This system also has several merits such as nontoxic processing, biocompatible and biodegradable materials, and mechanical properties that are comparable to scaffolds made by salt leaching.

In this study, we fabricated PCL scaffolds with interconnecting pores using a 3-D plotting system. We investigated the influence of pore geometry and scaffold architecture. Scanning electron microscopy (SEM), micro-computed tomography (μ-CT), and dynamic mechanical analysis (DMA) were used to characterize the morphology and mechanical properties of the resulting scaffolds. The cell responses on the scaffolds were observed by SEM and a laser scanning microscope.

2 Experimental

2.1 Materials and fabrication of the scaffolds

PCL (Catalog No. 440744) was obtained from Sigma-Aldrich (St. Louis, MO, USA). PCL has an average molecular weight (M_n) of 80,000 and a melting point of 60°C. Polymer pellets were melted at 100–130°C in a heating cylinder, and 3-D plotting scaffolds were made using the Bioplotter® System (Envisiontec GmbH, Gladbeck, Germany). The computer-controlled Bioplotter® can work under various materials and fabricating conditions such as shape, thickness, and space of strands. PCL was ejected through a heated nozzle, and the strand of PCL could be plotted as layer-by-layer deposition on a stage. To observe the effect of nozzle size and distance between strands, we fabricated three different groups. The groups were 200 (nozzle size)/300 (distance between strands) with 27 G, 250/500 with 25 G, and 330/700 μm with 23 G. As shown in Fig. 1, a 3-D cubic scaffold (10 × 10 × 5 mm^3) was plotted layer by layer with a plotter through the extrusion of melted PCL on a plate.

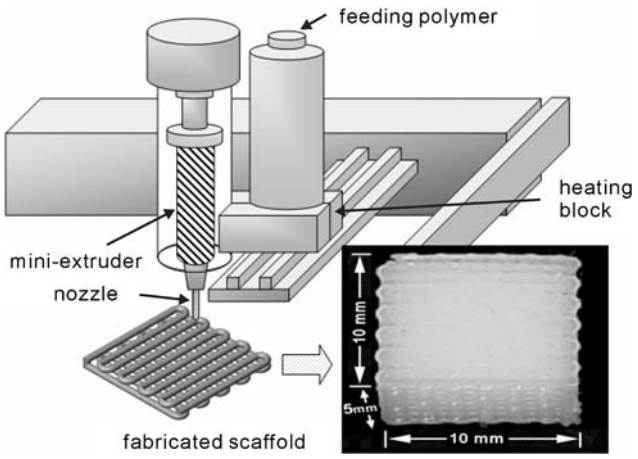

Fig. 1 Schematic of the 3-D melt-plotting technique

A salt-leaching PCL scaffold served as a control group to compare the various properties of the 3-D plotted scaffolds. To fabricate the salt leaching PCL scaffold, polymer pellets were dissolved into 10 ml of chloroform by stirring for several hours (~4 h) at room temperature. Ammonium bicarbonate (NH_4HCO_3) particles (~500 μm) were then added to the PCL solution. The weight ratio of salt to PCL was controlled at 7:1. The slurry of PCL/salt was put into a disk-type Teflon mold of 10 mm diameter and 5 mm thickness. Before the materials were fully solidified, they were pulled out from the Teflon mold and immersed in a citric acid solution (40% w/v) at room temperature to produce gas foaming and salt leaching simultaneously. To eliminate all the remaining salt, the samples were immersed in distilled water (~2 days). The samples were then kept in a dry oven until the experiments.

2.2 Characterization of scaffolds

The structural morphology of the fabricated scaffold was observed using μ-CT (Harmony 160H; DRGEM, Seoul, Korea) and SEM. The scanner was set to a voltage of 125 kV at a current of 120 μA to allow sufficient energy. Scaffolds were scanned at a 512 × 512 × 512 pixel resolution with an integration time of 120 ms to produce 3-D reconstructed images. In addition, 3-D morphologies of the scaffold were observed using SEM. They were coated with Pt and observed by SEM operating up to 15 kV.

The compressive modulus of the scaffolds was measured with a DMA Q800 (TA Instruments, New Castle, DE, USA) for various nozzle sizes, strand diameters, and pore sizes. The experiment was performed under conditions of an isothermal temperature/frequency sweep with the compression mode (strain = 2%) under an ambient temperature of 30°C. In measuring the compressive modulus using the DMA Q800, we applied a free load force of

0.1 N and a force track of 110%. The zig shape for DMA compressive testing was circular with a diameter of 15 mm.

2.3 Cell culture

The scaffolds were prepared in $10 \times 10 \times 5$ mm^3 for cell culture and were sterilized using 70% EtOH and UV light. The scaffolds were put in culture medium overnight. Chondrocytes were obtained using a 2% collagenase digestion method from porcine articular cartilage. Isolated chondrocytes were cultured in Dulbecco's modified Eagle's medium (DMEM) supplemented with 10% fetal bovine serum (FBS) and 1% penicillin/streptomycin. The cells were maintained up to passage 2 and were collected by trypsin-EDTA treatment. The cells were then seeded on scaffolds at a density of 5×10^5 cells/sample. The cell scaffolds were incubated in 5% CO_2 at 37°C and cultured for a period of 8 weeks. The medium was changed every other day. To inspect the detailed morphologies of cells on the scaffolds, SEM was used at 4 weeks and 8 weeks after seeding. The cell/scaffold constructs were fixed in 2.5% glutaraldehyde and dehydrated in a graded ethanol series. Dried scaffolds were coated with Au and examined under SEM at 15 kV.

2.4 Migration and attachment of chondrocytes into scaffolds

The migration of chondrocytes toward the middle region of various scaffolds and attachment of chondrocytes with strands were examined by staining chondrocytes using propodium iodine (PI), which specifically stains the nuclei of cells, or alexa-568 conjugated phalloidin (Invitrogen, Carlsbad, CA, USA). Alexa-568 conjugated phalloidin is an actin specific marker that reveals the cytoskeletal structure of chondrocytes. We fixed 4- and 8-week-old cell/scaffold constructs with 4% paraformaldehyde in 0.1 M phosphate buffer. The cell/scaffold constructs were embedded in 2 M sucrose in 0.1 M phosphate buffer to protect the cells from damage during cryofixation. The cell/scaffold constructs were then cryofixed by plunging into liquid nitrogen. Cryofixed cell/scaffold constructs were sectioned using a Cryostat 2000 (Leica, Solms, Germany) at −25°C and then washed with 0.2% Triton X-100 in 0.1 M phosphate buffer. Sectioned cell/scaffold constructs were stained with 1/3,000 diluted PI for 2 min or 1/200 diluted Alexa-568 conjugated phalloidin for 40 min at room temperature with shaking. Sections were washed three times and then mounted with Vectashield (Vector Laboratories, Burlingame, CA, USA). Cytoskeletal structures and nuclei of chondrocytes were examined under a laser scanning microscope (LSM510; Carl Zeiss, Oberkochen, Germany). Z-series sections were taken and then processed using the LSM image browser (Carl Zeiss) to reveal 45°C tilted views of the cell/scaffold constructs.

3 Results and discussion

μ-CT images were used to visualize the fabricated scaffolds and a salt-leached scaffold (Fig. 2). As shown in the figure, the plotted scaffolds showed regular, well structured shapes and good interconnected pores. The salt-leached scaffold, however, showed an irregular closed-pore structure. In addition, Fig. 3 shows that the 3-D plotted scaffolds had a highly porous structure, while that of the salt-leached scaffold was poorly interconnected.

Figure 4 shows the comparison of the designed strand period and measured strand period for various needle diameters: a 27 G (200 μm) needle plotted strand of 140, 240, and 340 μm period; a 25 G (250 μm) for 200, 300,

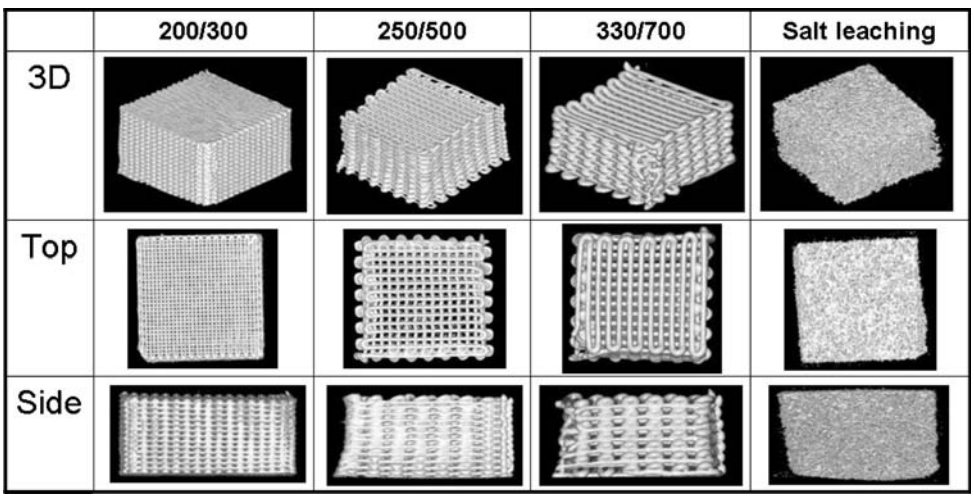

Fig. 2 μ-CT images of plotted (200/300, 250/500, and 330/700 μm) scaffolds and a salt-leached scaffold

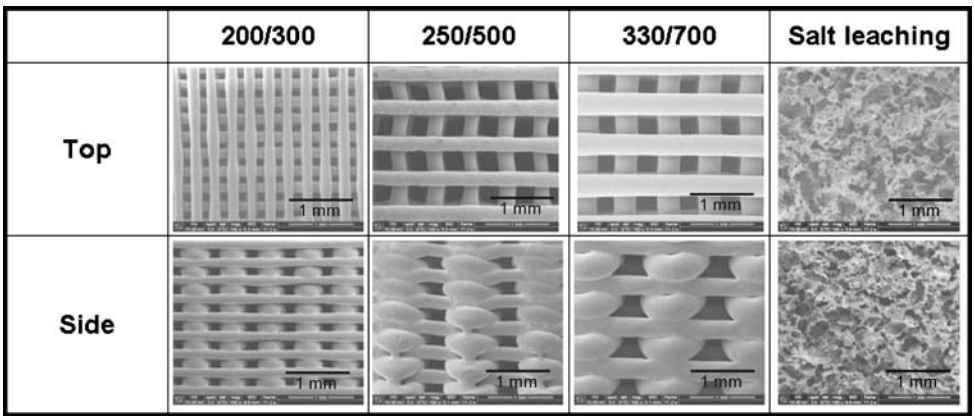

Fig. 3 SEM images of plotted (200/300, 250/500, and 330/700 μm) scaffolds and a salt-leached scaffold

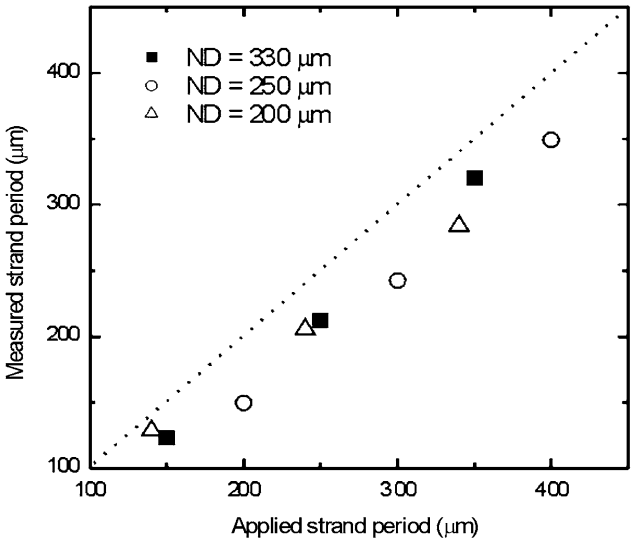

Fig. 4 Comparison of the designed strand period and measured strand period for various needle diameters

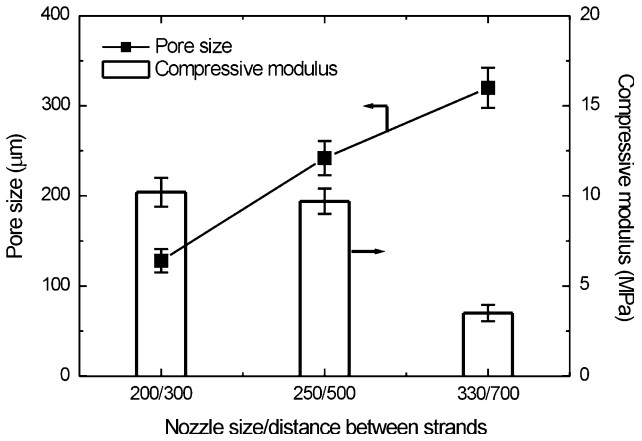

Fig. 5 Comparison of the compressive modulus in the 3-D PCL scaffolds for various nozzle size/distance between strands values and pore sizes

400 μm; and a 23 G (330 μm) for 150, 250, and 350 μm. The strand period of the cubic scaffold was measured under a microscope, and the manufacturing error of the fabricated scaffolds versus the designed scaffolds was within 3%. By using the strand period and strand diameter, the porosity of the fabricated scaffolds had a range of 45–75%.

The compressive modulus of the 3-D scaffold fabricated using a plotting method was tested with a dynamic mechanical analyzer. The variations in the modulus for the nozzle size and distance between strands were plotted in Fig. 5. A PCL salt-leached scaffold with a porosity of 82.4% and a pore size less than 500 μm had a compressive modulus of 0.2 MPa. The compressive moduli of the plotted scaffolds were in the range of 3.5–10.3 MPa for 128–320 μm pores size. Although comparing the compressive moduli of the plotted and salt-leached scaffolds directly is difficult, the modulus of the plotted scaffolds is clearly superior to that of a conventional scaffold produced by the salt-leaching method. The result of the mechanical test indicates that the plotted scaffolds have the obvious advantage that their mechanical properties can be easily manipulated by adjusting the scaffold geometry.

Figure 6a shows the SEM images of the top views of the cell/scaffold constructs. At 4 weeks of seeding, the cells had spread over the plotted scaffold surface, and cellular bridging between adjacent strands occurred in the corners of the pores. After 8 weeks, the cells on the scaffold formed a dense cellular covering over the surface, and the formation of a dense cellular network filled the complete porous space of the scaffold. However, as shown in the top view of the Fig. 6a, in the large pore sized scaffold (330/700), the cells are not enough covering the scaffold. The cells on the salt-leached scaffold only partially covered the surface over the 8-week time period. Figure 6b presents side views of the cell/scaffold constructs. The cells on the plotted scaffolds had formed more confluent pores over the 8 weeks, whereas the salt-leached scaffold only partially covered the surface. The cells on the plotted scaffold migrated and attached through the interconnected pores of the scaffolds, and at 4 weeks, the cells started filling up the

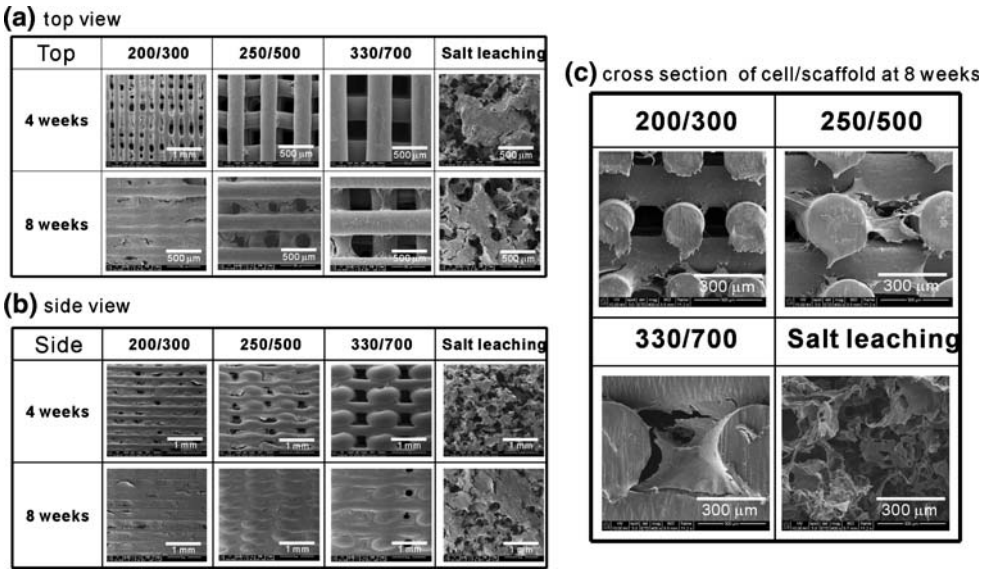

Fig. 6 SEM images of plotted (200/300, 250/500, and 330/700 μm) scaffolds and a salt-leached PCL scaffold cultured for 4 and 8 weeks. (**a**–**c**) Present top, side, and cross section views of the scaffolds, respectively

pores of the plotted scaffolds. A salt-leached scaffold with non-connected pores does not allow cell ingrowth into the scaffold. After 8 weeks, most of the plotted scaffold surfaces were filled with cells. Figure 6c presents the cross sections of cell/scaffold constructs at 8 weeks. As shown in the figure, the plotted scaffolds induce the cell penetration among the strands. However, the cell penetration can not be observed in the salt leaching scaffold.

Another important requirement of a 3-D scaffold for tissue engineering is that the scaffold must allow seeded chondrocytes to migrate toward the middle regions of the scaffold easily, and the migrated cells must be able to attach to the strands. Using cell-specific markers, such as PI for the nucleus of cells and phalloidin for actin cytoskeletal structures, the penetration and attachment of chondrocytes in the middle regions of the scaffolds were examined. Figure 7 shows the cell attachment on the surface of the strands and cellular compactness between the strands. As shown in Fig. 7, at 8 weeks, the cells on the plotted scaffolds had proliferated on the strands and filled the scaffold pores. The cells cultured on the plotted scaffold formed a dense cell layer covering the surfaces,

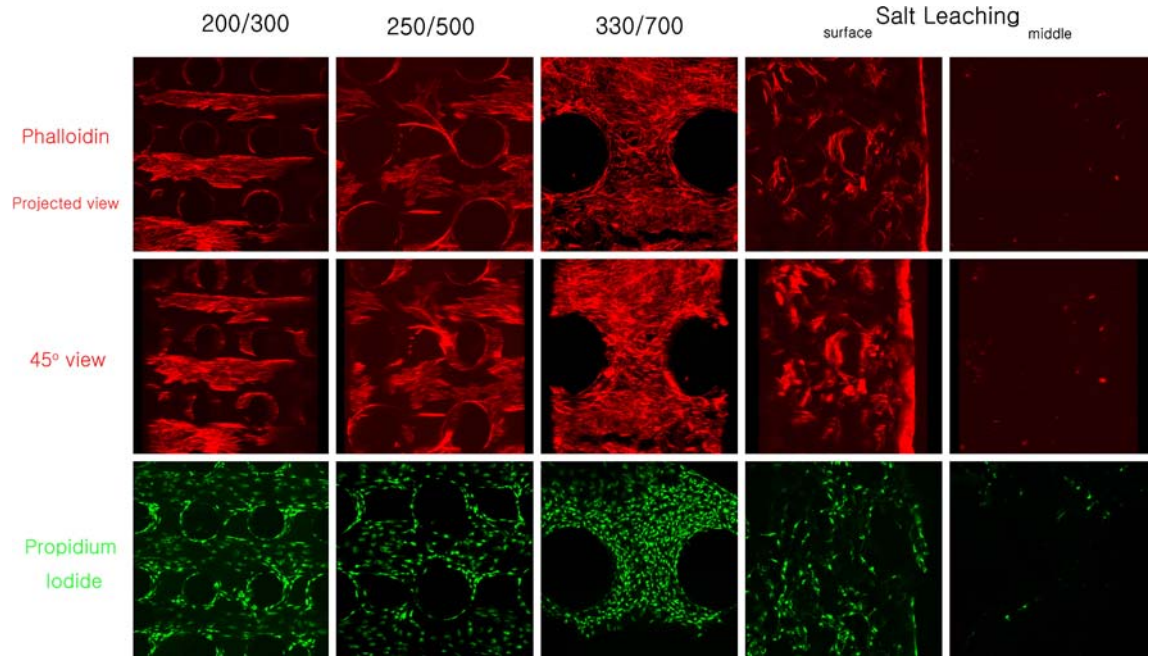

Fig. 7 Comparison of cell attachment and compactness of the scaffolds (200/300, 250/500, and 330/700 μm) fabricated using a 3-D plotter and a salt-leached scaffold

whereas those cultured on the salt-leached scaffold formed a cell monolayer that only partially covered the surfaces. In the cross section, the cells on the 330/700 scaffold were denser than those on the 200/300 scaffold because the cells more easily penetrated into the large pores between the strands. The PCL strands for the small pore size were too hydrophobic, so the cells could not spread out in the space between the strands.

Based on the results, we found that the plotted scaffolds provided more opportunity for cells to penetrate into the scaffold than a salt-leached scaffold and conclude that the plotted method is more suitable for scaffolds used in cartilage regeneration than a conventional salt-leached scaffold.

4 Conclusions

In this study, we used a 3-D Bioplotter® System to fabricate scaffolds with an interconnected structure. The scaffolds fabricated by the 3-D plotting method were formed to induce cell penetration for cell ingrowth. The interconnected structure of the scaffold will be optimal for allowing nutrient inflow and metabolic waste outflow. We confirmed the uniform structure of the 3-D scaffold with the strand pattern and observed the compressive modulus and cellular response. The plotted 200/300 scaffold presented a high compressive modulus; the dense scaffold with thick strands also presented a high compressive modulus, and the sparse scaffold (300/700) was suitable for cell ingrowth. The plotted scaffold was more suitable for cell ingrowth than a salt-leached scaffold.

References

1. D.W. Hutmacher, T. Schantz, I. Zein, K.W. Ng, S.H. Teoh, K.C. Tan, J. Biomed. Mater. Res. **55**, 203 (2001). doi:10.1002/1097-4636(200105)55:2<203::AID-JBM1007>3.0.CO;2-7
2. T.B.F. Woodfield, J. Malda, J. de Wijn, F. Péters, J. Riesle, C.A. van Blitterswijk, Biomateriasls **25**, 4149 (2004). doi:10.1016/j.biomaterials.2003.10.056
3. E. Sachlos, J.T. Czernuszka, Eur. Cell Mater. **5**, 29 (2003)
4. X. Wang, Y. Yan, R. Zhang, Trends Biotechnol. **25**, 505 (2007). doi:10.1016/j.tibtech.2007.08.010
5. A. Pfister, R. Landers, A. Laib, U. Hübner, R. Schmelzeisen, F. Mülhaupt, J. Polym. Sci. Part A **42**, 624 (2004). doi:10.1002/pola.10807
6. S.J. Hollister, Nat. Mater. **4**, 519 (2005). doi:10.1038/nmat1421
7. M.E. Hoque, D.W. Hutmacher, W. Feng, S. Li, M.-H. Huang, M. Vert et al., J. Biomater. Sci. Polym. Ed. **16**, 1595 (2005). doi:10.1163/156856205774576709
8. H. Seitz, W. Rieder, S. Irsen, B. Leukers, C. Tille, J. Biomed. Mater. Res. Part B **74B**, 782 (2005). doi:10.1002/jbm.b.30291
9. M. Lee, J.C.Y. Dunn, B.M. Wu, Biomaterials **26**, 4281 (2005). doi:10.1016/j.biomaterials.2004.10.040
10. W. Mironov, T. Boland, T. Trusk, G. Forgacs, R.R. Maikwald, Trends Biotechnol. **21**, 157 (2003). doi:10.1016/S0167-7799(03)00033-7
11. J.M. Williams, A. Adewunmi, R.M. Schek, C.L. Fanangan, P.H. Krebsbach, S.E. Feinbergh et al., Biomaterials **26**, 4817 (2005). doi:10.1016/j.biomaterials.2004.11.057
12. G. Vozzi, C. Flaim, A. Ahluwalia, S. Bhatia, Biomaterials **24**, 2533 (2003). doi:10.1016/S0142-9612(03)00052-8
13. I. Zein, D.W. Hutmacher, K.C. Tan, S.H. Teoh, Biomaterials **23**, 1169 (2002). doi:10.1016/S0142-9612(01)00232-0
14. R. Landers, U. Hübner, R. Schmelzeisen, R. Mülhaupt, Biomaterials **23**(2203), 4437 (2002)
15. J.-T. Schantz, A. Brandwood, D.W. Hutmacher, H.L. Khor, K. Bittner, J. Mater. Sci. Mater. Med. **16**, 807 (2005). doi:10.1007/s10856-005-3584-3
16. B. Partee, S.J. Hollister, S. Das, J. Manufac, Sci. Eng. **128**, 531 (2006)